ELSEVIER

Journal of Chromatography A, 776 (1997) 15–30

JOURNAL OF CHROMATOGRAPHY A

Kinetic analysis of the interaction between the monoclonal antibody A33 and its colonic epithelial antigen by the use of an optical biosensor
A comparison of immobilisation strategies

B. Catimel[a], M. Nerrie[a], F.T. Lee[b], A.M. Scott[b], G. Ritter[c], S. Welt[c], L.J. Old[c], A.W. Burgess[a], E.C. Nice[a,*]

[a]*Ludwig Institute for Cancer Research, PO Royal Melbourne Hospital, Parkville, Victoria 3050, Australia*
[b]*Joint Oncology Unit, Ludwig Institute for Cancer Research and Austin Hospital, Heidelberg, Victoria 3084, Australia*
[c]*Ludwig Institute for Cancer Research, New York Unit at Memorial Sloan-Kettering Cancer Center, New York, NY 10021, USA*

Abstract

The interaction between the humanised A33 monoclonal antibody and the corresponding $F(ab)'_2$ or Fab' fragments with the colonic epithelial A33 antigen, purified by micropreparative HPLC from membrane extracts of the colonic carcinoma cell line LIM 1215, has been studied with the BIAcore 2000 biosensor using surface plasmon resonance detection. The surface orientation of immobilised antibody and the Fab' fragment onto the biosensor surface was controlled using alternative immobilisation chemistries. This resulted in significantly higher molar binding activities compared with the conventional N-hydroxysuccinimide (NHS)/N-ethyl-N'-dimethylaminopropylcarbodiimide (EDC) chemistry. This increase in signal resulted in a concomitant increase in sensitivity of detection, which facilitates analysis of low levels of A33 antigen. The apparent association rate (k_a) and dissociation rate (k_d) constants obtained with the different immobilisation chemistries were determined. These analyses showed that the kinetic constants obtained for the IgG were not significantly affected by the method of immobilisation. $F(ab)'_2$ and Fab' fragments immobilised using NHS/EDC chemistry showed significantly lower apparent affinity. By contrast the use of the thiol coupling chemistry with the Fab' fragment gave a five fold increase in observed K_A, resulting in a similar affinity to that observed with the intact IgG molecule. © 1997 Elsevier Science B.V.

Keywords: Antibody immobilisation; Immobilisation; Kinetic studies; Biosensors; Detection, LC; Monoclonal antibodies; Antigens; Immunoglobulins; Proteins

1. Introduction

Recent advances in biosensor technology [1] have led to the development of an optical biosensor (BIAcore) capable of measuring biospecific interactions in real time as well as allowing detailed investigation of the reaction kinetics [2,3]. This biosensor technology uses the optical detection principle of surface plasmon resonance [4], a technique which measures small changes in refractive index at, or near to, the gold sensor surface [5]. Thus the change in mass as a ligand binds to, or dissociates from, its binding partner can be readily monitored. Binding studies can be performed by

*Corresponding author.

0021-9673/97/$17.00
PII S0021-9673(97)00087-3

covalently attaching one interactant [monoclonal antibody (mAb), protein, peptide or DNA] onto the sensor and flowing reagents of interest (purified proteins, chromatographic fractions, tissue culture media, etc.) over this surface.

We are currently using this biosensor technology to investigate the interaction between the A33 monoclonal antibody [6–8] and its colonic epithelial antigen [9]. The monoclonal antibody A33, which is currently being used in phase I/II radioimmunotherapy [7,8], detects a novel intestinal antigen which is present on normal and transformed epithelium [6]. The A33 antigen, which has an apparent molecular mass of 43 000, has recently been purified to homogeneity [9] from membrane extracts of the LIM1215 colonic carcinoma cell line [10] using a combination of multidimensional HPLC coupled with BIAcore analysis of the chromatographic fractions [11]. Final purification to homogeneity (1–2 $\mu g/10^9$ cells) was achieved using reversed-phase (RP) HPLC, but this procedure was shown by biosensor analysis to cause partial denaturation [9].

In the studies reported herein, the A33 ligand [9] was purified to homogeneity under non-denaturing conditions using a modification of the previously described chromatographic protocol [9] involving affinity chromatography [12], micropreparative anion-exchange and size-exclusion chromatography (SEC) [13–15]. RP-HPLC was only used analytically to monitor sample purity.

Using this material, we have investigated two alternative conjugation protocols for stable immobilisation of IgG or Fab′ fragments onto the biosensor surface in a defined orientation. In the first method, humanised A33 IgG [16] was bound by the Fc region to Protein-A immobilised onto the sensor surface, and then cross-linked in situ using dimethyl pimelimidate dihydrochloride [17]. To immobilise the humanised A33 Fab′ in a defined orientation, the Fab′ fragment was thiol conjugated using Ellman's reagent by the sulphydryl of the hinge region [18] to reduced cystamine immobilised onto the sensor surface. A comparison of relative surface activities and the kinetic rate constants obtained for A33 IgG, $F(ab')_2$ and Fab′ fragments using these alternative immobilisation procedures is presented. Data obtained with the conventional NHS/EDC chemistry has been used for comparison.

2. Materials and methods

2.1. A33 antigen purification

2.1.1. Triton X-114 extraction of LIM1215 cells

Triton X-114 extracts of LIM1215 colonic carcinoma cells were prepared as described previously [9]. The detergent phase, containing the A33 antigen, was taken for chromatographic purification.

2.1.2. Affinity chromatography

An A33 affinity column was prepared by conjugating murine A33 monoclonal antibody [6] to Protein A-Sepharose CL4B (Pharmacia Biotech, Uppsala, Sweden) with 20 m*M* dimethyl pimelimidate dihydrochloride (ICN Biochemicals, Costa Mesa, CA, USA) according to the protocol of Schneider et al. [17]. Non-covalently bound antibody was removed with 50 m*M* glycine (pH 2.5). Residual active dimethyl pimelimidate groups were deactivated by washing with 0.1 *M* ethanolamine (pH 8.0). The affinity support was then equilibrated with phosphate-buffered saline (PBS; pH 7.4) containing 0.05% (w/v) 3-[(cholamidopropyl)di-methylamino]-1-propanesulfonate (CHAPS).

The Triton X-114 detergent phase was diluted 5-fold with PBS, 0.05% CHAPS (pH 7.4) and incubated overnight at 4°C with the A33 IgG-Protein-A. The packing was then poured into an empty HR 10/10 column and attached to an fast protein liquid chromatography (FPLC) system (Pharmacia Biotech).

The column was washed (20 column volumes), at a flow-rate of 0.5 ml/min, with PBS, 0.05% CHAPS (pH 7.4) followed by a wash with PBS, 0.05% CHAPS (pH 5.0). Bound proteins, including the A33 antigen, were then eluted with 50 m*M* glycine (pH 2.5). The elution profile was monitored at 280 nm.

2.1.3. Anion-exchange chromatography

The A33 antigen containing fraction eluted from the affinity column was diluted two-fold with 20 m*M* Tris–HCl (pH 7.5), 0.005% (v/v) Tween 20, adjusted to pH 7.5 with 1 *M* Tris–HCl (pH 9.0) and injected onto a Mono Q PC 1.6/5 micropreparative anion-exchange column connected to a SMART system (Pharmacia Biotech). Proteins were eluted with a linear 60 min gradient to 1 *M* NaCl at a

flow-rate of 100 μl/min. Detection was performed at 215 nm and 100 μl fractions were collected automatically. The A33 antigen in eluant fractions was detected using both biosensor analysis with humanised A33 $F(ab)'_2$ immobilised on the sensor surface and Western blot analysis under non-reducing conditions, as reported previously [9].

2.1.4. Size-exclusion chromatography (SEC)

Active fractions eluted from the Mono Q column (800 μl) were pooled and individual 100-μl aliquots loaded onto a Superose 12 HR 3.2/30 micropreparative size-exclusion column connected to the SMART system and equilibrated with PBS, 0.005% Tween 20. The column was eluted at a flow-rate of 100 μl/min. Detection was performed at 215 nm and 100 μl fractions were collected. The A33 antigen in eluate fractions was detected as in Section 2.1.3.

The protein concentration of the purified A33 antigen was calculated from the chomatographic peak area compared with an ovalbumin standard chromatographed under identical conditions (215 nm detection). The sample purity was determined by sodium dodecyl sulfate–polyacrylamide gel electrophoresis (SDS-PAGE) with silver staining (1-μl aliquot) and RP-HPLC (25-μl aliquot) of a pool of the size-exclusion purified material using a Brownlee Aquapore RP300 micropreparative RP-HPLC column (100×1 mm I.D.) as described previously [9].

2.2. Preparation and purification of humanised A33 monoclonal antibody and $F(ab)'_2$ fragment

Humanised A33 monoclonal antibody [16] was purified using Protein-A affinity chromatography. $F(ab)'_2$ were obtained by pepsin digestion [19] and purified by SEC on a Sephacryl S-200 (60×2.8 cm) column (Pharmacia Biotech) which had been equilibrated with 50 m*M* sodium phosphate (pH 7.4) containing 0.15 m*M* NaCl. Elution was performed at a flow-rate of 0.5 ml/min. Prior to immobilisation onto the biosensor, A33 IgG and $F(ab)'_2$ were repurified by micropreparative SEC using a Superose 12 HR 3.2/30 column connected to a SMART system to ensure homogeneity. Fractions were analysed by SDS-PAGE under non-reducing conditions with Coomassie blue R250 staining.

2.3. Preparation and purification of Fab′ fragment

$F(ab)'_2$ fragments, generated as described in Section 2.2 (0.7 mg/ml, 100 μl), were reduced with 5 m*M* 2-mercaptoethanolamine at 37°C [18]. The reduction was monitored by injecting aliquots (25 μl) onto the Superose 12 HR 3.2/30 micropreparative SEC system and found to be complete after 30 min. 5,5′-Dithiobis-(2-nitrobenzoic acid) (DTNB, Ellman's reagent, ICN Biochemicals) was then added (final concentration 10 mg/ml) and incubated for 30 min at 37°C in order to protect the Fab′ sulphydryl group [18]. Any residual sulphydryl groups were blocked with 30 m*M* iodoacetamide. The A33 Fab′-TNB fragment was purified by micropreparative SEC as described in Section 2.1.4.

2.4. Western blot analysis

Electrophoresis and Western blot analyses were performed using precast Phastgels in a Phastsystem (Pharmacia Biotech) as described [9].

2.5. Biosensor analyses

Biosensor analyses were performed using a BIAcore 2000 (Pharmacia Biosensor, Uppsala, Sweden). Sensor chip CM5, surfactant P20 (a 10% solution of the non-ionic detergent Tween 20), the amine coupling reagents [N-hydroxysuccinimide (NHS), N-ethyl-N′-dimethylaminopropylcarbodiimide (EDC) and ethanolamine] and the thiol reagent were also obtained from Pharmacia Biosensor. Humanised A33 monoclonal antibody, $F(ab)'_2$ and F(ab)′ fragments were immobilised onto the biosensor surface using the protocols described in Section 2.6. Chromatographic fractions and purified A33 antigen were diluted in BIAcore buffer [HBS: 10 m*M* 4-(2-hydroxyethyl)-1-piperazineethanesulfonic acid (HEPES; pH 7.4) containing 3.4 m*M* EDTA, 0.15 m*M* NaCl and 0.005% (v/v) Tween 20] prior to analysis. Samples (30 μl) were injected over the sensor surface at a flow-rate of 5 μl/min. Following completion of the injection phase, dissociation was monitored in BIAcore buffer for 360 s at the same flow-rate. The bound antigen was eluted, and the surface regenerated between injections, using 40 μl of 10 m*M* NaOH. This treatment did not denature

the antibody or antibody fragments immobilised onto the sensor surface as shown by equivalent signals on re-injection of the ligand.

In order to investigate the possibility of rebinding of ligand during the dissociation process a modification of the BIAcore 2000 software (coinject) was used in some experiments in which excess soluble antibody (200 μg/ml and 1 mg/ml) was injected directly following the cessation of the ligand injection [20].

2.6. Conjugation of antibody and antibody fragments onto the biosensor surface

2.6.1. IgG, F(ab)$'_2$ and Fab' immobilisation using amine coupling

Humanised A33 IgG, A33 F(ab)$'_2$ and Fab' (40 μg/ml) were immobilised using N-ethyl-N'-dimethylaminopropyl-carbodiimide (EDC) and N-hydroxysuccinimide (NHS) as described previously [9].

2.6.2. Cross-linking of IgG onto immobilised Protein-A: orientation via the Fc portion of the molecule

Protein-A (ICN Biochemicals) was first immobilised onto the sensor surface using the NHS/EDC chemistry described in Section 2.6.1. 50 μl of Protein-A [400 μg/ml in 0.1 *M* sodium acetate buffer (pH4.0)] was injected at 2 μl/min over the activated surface. After coupling, the surface was deactivated by injection of 35 μl of 0.1 *M* ethanolamine (pH 8.0).

Humanised A33 IgG [50 μl, 50 μg/ml in 0.1 *M* sodium borate buffer (pH 9.2)] was then injected over the immobilised Protein-A. Bound IgG was cross-linked in situ to the Protein-A by injection of 100 μl of dimethyl pimelimidate dihydrochloride [50 m*M* in 0.1 *M* sodium borate buffer (pH 9.2)] at a flow-rate of 2 μl/min. The surface was then washed sequentially with 50 μl of 25 m*M* glycine (pH 2.5) (dissociation of non cross-linked IgG and Protein-A), 10 m*M* NaOH (used in binding experiments to dissociate antibody–ligand to regenerate the surface between experiments) and 0.1 *M* ethanolamine (pH 8.0) (deactivation of the cross linker).

2.6.3. F(ab)' immobilisation using thiol coupling: orientation by the sulphydryl at the hinge region of the F(ab)' fragment

Cystamine dihydrochloride (Sigma, St. Louis, MO, USA) (40 μl, 40 m*M* in 0.1 *M* sodium borate buffer, pH 8.5) was immobilised onto the biosensor surface using NHS/EDC chemistry. The immobilised cystamine was then reduced by injection of 40 μl 0.1 *M* dithiothreitol (DTT) in borate buffer at 4 μl/min. The Fab'-TNB, purified as described in Section 2.6.1, was diluted to 50 μg/ml in 0.1 *M* sodium acetate buffer (pH 4.0) in order to allow pre-concentration onto the biosensor surface. The Fab'-TNB was coupled onto the reduced cystamine at a flow-rate of 2 μl/min.

Residual reduced cystamine was deactivated by injection of 20 m*M* 2-(2-pyridinyldithio)ethaneamine hydrochloride (PDEA) (Pharmacia Biosensor) in 0.1 *M* sodium acetate (pH 4.0) containing 0.1 *M* NaCl (40 μl at 4 μl/min). The remaining TNB active groups were blocked by injection of 2.5 m*M* cysteine in sodium formate (pH 4.5) (40 μl at 4 μl/min).

2.7. Kinetic analysis of the biosensor data

In this study we have used both linear transformation (LR) [2,21] and non-linear least squares regression analysis (NLLS) [3] of the biosensor curves to estimate the apparent association (k_a) and dissociation (k_d) rate constants. A valency of 1 has been assumed for the A33 antigen.

For LR analysis data were manipulated using the BIA Evaluation kinetics evaluation package supplied by the manufacturer. For NLLS analysis sensorgram data were either saved as a text file and imported into ORIGIN (Micro Cal Software, MA, USA), or analysed using the BIA Evaluation version 2.1 software (Pharmacia Biosensor) into which the appropriate equations had been installed [22].

The goodness of fit between experimental data and fitted curves was estimated for linear fitting routines from the coefficient of correlation, R^2, and for non-linear least squares fitting by chi-squared analysis using the equation given below:

$$\chi^2 = \frac{\sum_1^n (r_f - r_x)^2}{n - p}$$

where r_f is the fitted value at a given point, r_x is the experimental value at the same point, n is the number of data points and p is the number of degrees of freedom.

To enable a comparison of the surface reactivity following the different immobilisation chemistries, the molar binding activities were calculated from the equation:

$$\text{Molar binding activity} = \frac{(\text{antigen response}) \times (\text{antibody molecular mass})}{(\text{amount of immobilised antibody}) \times (\text{antigen molecular mass})}$$

3. Results and discussion

3.1. A33 antigen purification

The small quantities of A33 antigen, purified as described previously [9], were not ideally suited for a detailed kinetic analysis of the A33 mAb–ligand interaction. Furthermore, it was established that the protein recovery from the final RP-HPLC step was approximately 45% whilst the recovery of biological activity was only 23%, suggesting both on-column protein losses and partial denaturation of the ligand during this chromatographic procedure [9]. Consequently, an alternative purification protocol has now been designed, which avoids the use of RP-HPLC, in order to obtain highly purified A33 antigen under mild non-denaturing conditions in sufficient quantities to perform detailed kinetic analyses.

The A33 antigen in Triton X-114 detergent extracts of LIM1215 colon carcinoma cells was purified by affinity chromatography followed by micropreparative anion-exchange HPLC on Mono Q PC 1.6/5 (results not shown). The active Mono Q fraction was further purified by micropreparative SEC on a Superose 12 HR 3.2/30 column (Fig. 1A). The A33 antigen was detected by biosensor analysis in the major peak eluting between 9 and 12 min (Fig. 1A). The sample purity of the pool of the active fractions from the size exclusion HPLC was determined by SDS-PAGE analysis using silver staining and analytical RP-HPLC using Brownlee Aquapore RP300 (100×1 mm I.D.) (Fig. 1B). The A33 antigen eluted, as shown by Western blot analysis (M_r 43 000 band, Fig. 1B, inset), in a symmetrical peak eluting around 51.8 min. Protein concentration was calculated from the peak area of the chromatographic trace obtained from the SEC (215 nm detection) compared with an accurately quantitated ovalbumin standard, which has a similar molecular mass to the A33 antigen, chromatographed under identical conditions. Approximately 4 μg of A33 antigen was purified to homogeneity from each preparation ($2 \cdot 10^9$ LIM1215 cells), with a purity greater than 95%, giving sufficient material to perform detailed kinetic analyses. This yield was almost four times that which had been achieved with our original purification scheme [9].

Preliminary attempts to immobilise the purified ligand onto the sensor surface using NHS/EDC chemistry resulted in a loss of reactivity with the conformationally dependent A33 monoclonal antibody. This surface was, however, recognised by a polyclonal antisera against the N-terminal sequence (residues 2–20) of the purified ligand [9]. Therefore, we decided to immobilise the A33 antibody or antibody fragments and to perform kinetic studies by injecting purified ligand in a continuous flow over the multiple sensor surfaces. An additional advantage with this format is that analysis is not complicated by the bivalency of IgG and $F(ab')_2$ [21]. A valency of 1 was assumed for the A33 ligand, although it should be noted that on SEC and native PAGE the molecule has an apparent molecular mass of approximately 180 000, suggesting that it may form a tetrameric complex [9].

3.2. Characterisation of A33 monoclonal antibody, $F(ab)'_2$ and Fab′ fragments

The homogeneity of the antibody preparation used for immobilisation onto the sensor chip is fundamental for successful kinetic analysis [11]. Purified humanised A33 IgG, $F(ab')_2$, Fab′ and TNB-Fab′ were analysed by micropreparative SEC using Superose 12 HR 3.2/30 and SDS-PAGE under non-reducing conditions prior to immobilisation onto the biosensor (results not shown). The preparations were shown to be homogeneous by these criteria. The TNB-Fab′ was found to be stable at 4°C and could be used for multiple immobilisations.

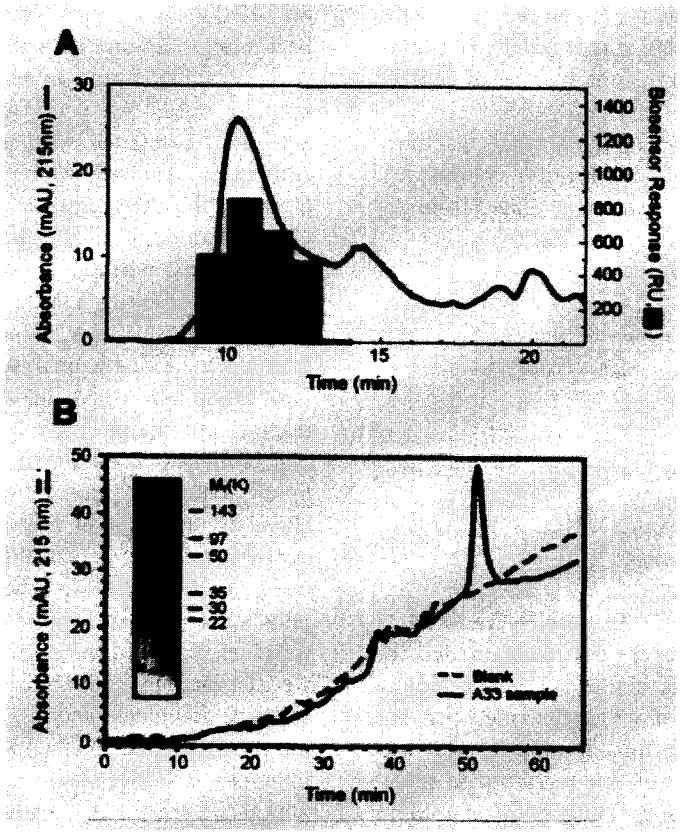

Fig. 1. Purification and characterisation of the A33 antigen. (A) Size-exclusion chromatography: Mono-Q active fractions (100-μl aliquots) were applied to a Superose 12 HR 3.2/30 micropreparative size-exclusion column equilibrated with PBS, 0.005% Tween 20 (see Section 2.1.4). The column was eluted at a flow-rate of 100 μl/min and 100 μl fractions were collected. An aliquot (10 μl) was taken for biosensor analysis. A positive response was only found in fractions 8–13. (B) Microbore RP-HPLC analysis of Superose 12 fractions: the homogeneity of the Superose 12 active fractions (pool 9–12 min (A), 25 μl-aliquot) was analysed by RP-HPLC using a Brownlee RP 300 column (100×1 mm ID) equilibrated with 0.15% trifluoroacetic acid (TFA). The protein was eluted with a linear 60 min gradient to 60% aqueous *n*-propanol–0.125% TFA. The identity of the major peak, eluting at 51.8 min was confirmed by Western blot analysis under non-reducing conditions using mAb A33 (shown inset). A corresponding aliquot from a blank run on the Superose 12 column was taken for comparaison (- - -).

3.3. Biosensor immobilisation

The most generally used technique for covalent immobilisation of proteins or peptides surface via primary NH_2 groups (amino-terminus or lysine residues) onto the carboxymethyldextran-modified gold sensor surface involves activation of the carboxylic group using NHS/EDC chemistry [23–25]. However, heterogeneity can be introduced during the coupling procedure itself [11,26]. Such random immobilisation may cause loss, or reduction, of biological activity by coupling near the antigen binding site and may therefore give rise to heterogeneous and complex kinetics.

As well as the NHS/EDC chemistry, several other strategies have been used previously to immobilise antibody molecules onto the sensor surface. Chemical coupling has been achieved by the formation of disulfide bonds between immobilised cystamine dihydrochloride and antibody modified by a thiol coupling agent such as N-succimidyl-3-(2-pyridyldithio)propionate (SPDP) [27]. However, this thiol coupling involved derivatisation of the antibody via primary amino groups with SPDP which, as we

have discussed in Section 3.2 for the NHS/EDC chemistry, can result in random orientation of the IgG molecule. In an alternative approach, aldhehyde coupling has been used to immobilise antibody via carbohydrate chains following oxidation onto an hydrazine-activated sensor surface [25,27] but this may also induce multiple site attachment.

Capture techniques, often involving the incorporation of a specific functional group into the protein to be immobilised, have also been used following immobilisation of a suitable primary reagent using the NHS/EDC chemistry. Such techniques ideally rely on the generation of a biological interaction with limited dissociation ($k_d < 10^{-6}$ s^{-1}), in order to avoid losses from the sensor surface during subsequent binding experiments. Since the biotin–avidin interaction has very high affinity ($K_D = 10^{-15}$ M), antibodies have been biotinylated and then immobilised onto a Streptavidin derivatised sensor surface [25,27]. However, the antibody was derivatised via primary amino groups using NHS-biotin [27], which as we have discussed above for the NHS/EDC and SPDP chemistries, will result in random orientation of the IgG molecule.

Rabbit anti-mouse (RAM) Fc antibody or subclass specific antibodies (e.g., RAM-IgG1) can be first immobilised via NHS/EDC chemistry in order to capture mouse IgG [28,29]. This has been used, in particular, in epitope mapping strategies. As discussed above, the interaction between the rabbit anti-mouse Fc antibody and the monoclonal antibody needs to be of high affinity in order to avoid dissociation between the two antibodies during the binding experiments. Protein-A can also be immobilised onto the sensor surface via NHS/EDC chemistry in order to capture antibodies via their Fc domain [30]. However subsequent bleeding of the antibody from Protein-A can interfere with antigen binding experiments and additionally the regeneration step may dissociate the IgG from the Protein-A.

We have therefore devised alternative immobilisation strategies for IgG or Fab' fragments giving stable surfaces in a defined orientation (Fig. 2). To ensure the reproducible generation of sensor surfaces, immobilisations were performed automatically in situ using the BIAcore 2000 control software.

3.4. Cross-linking of A33 IgG onto immobilised Protein-A: orientation via the Fc portion of the molecule

Protein-A was first immobilised onto the sensor

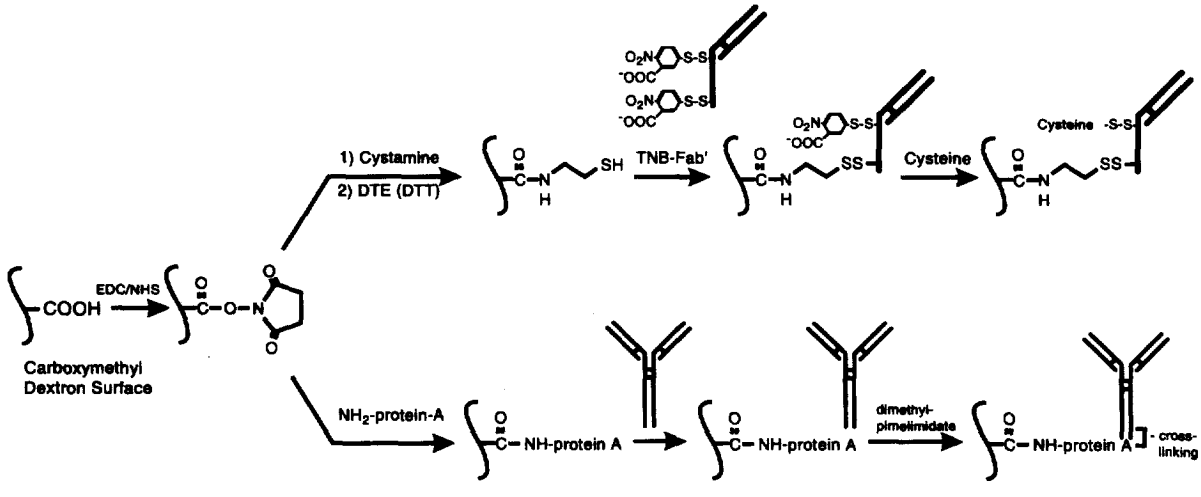

Fig. 2. Immobilisation strategies for surface orientation of IgG and Fab': Protein-A or cystamine were immobilised onto the sensor surface using NHS/EDC chemistry. The humanised A33 IgG was bound by the Fc region to Protein-A immobilised onto the sensor surface (lower pathway), and then cross-linked in situ using dimethyl pimelimidate dihydrochloride. The humanised A33 Fab', derivatised with Ellman's reagent, was thiol conjugated by the sulphydryl of the hinge region to reduced cystamine immobilised onto the sensor surface (upper pathway). Residual TNB groups were deactivated with cysteine.

surface using NHS/EDC chemistry (Figs. 2 and 3A). A signal of approximately 10 000 RU, corresponding to approximately 10 ng/mm^2 Protein-A immobilised onto the sensor surface [31], was obtained. A33 mAb was then injected over this surface (Fig. 3B) and, following binding to the immobilised Protein-A, was cross-linked in situ using dimethyl pimelimidate dihydrochloride (Figs. 2 and 3B). Following removal of non cross-linked IgG and deactivation of remaining dimethyl pimelimidate, a net increase in detector signal of 3454 RU resulted due to the cross-linked antibody (Fig. 3B). The level of IgG immobilisation could be modulated by varying the IgG concentration and injection time. After cross-linking, the affinity surface was stable to exposure to low (pH 2.5) or high (pH 11) pH and no significant loss of antibody (as evidenced by a decrease in immobilised RU) was observed during the multiple cycles performed. In contrast, when the cross-linker was omitted, complete dissociation of the Protein-A–mAb complex was observed following low or high pH washes (data not shown).

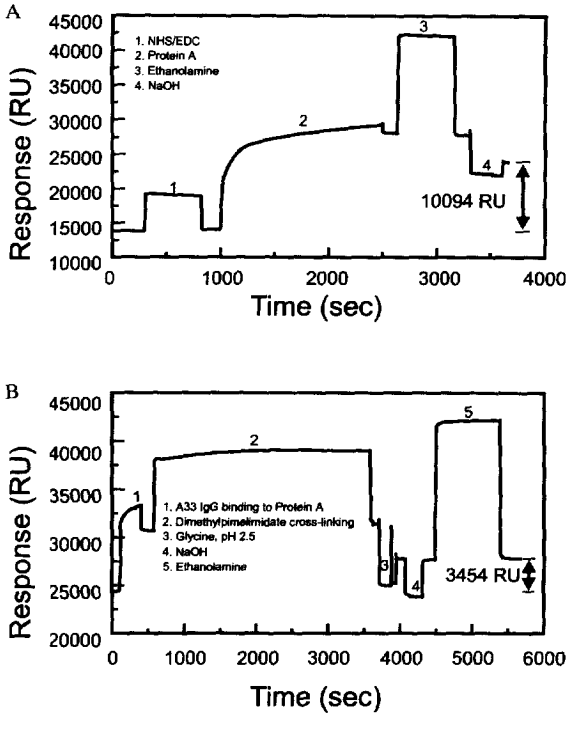

Fig. 3. Immobilisation of IgG by cross-linking in situ to Protein-A. (A) Protein-A was immobilised on the carboxymethyldextran-modified gold sensor surface using NHS/EDC chemistry. The individual stages are indicated (1–4). The signal due to covalently bound Protein-A is 10 094 RU. (B): Following immobilisation of Protein-A (A), the humanised IgG was injected over the surface and cross-linked in situ as indicated (stages 1, 2). After washing (stages 3, 4) and deactivation (stage 5), an overall increase in signal of 3454 RU, corresponding to cross-linked A33 IgG was obtained.

3.5. Fab′ immobilisation using thiol coupling: orientation by the sulphydryl of the hinge region of the Fab′ fragment

Cystamine dihydrochloride was immobilised onto the biosensor surface using the conventional NHS/EDC chemistry (Figs. 2 and 4). After reduction of the cystamine in situ the purified Fab′-TNB was injected and conjugated by thiol coupling onto the immobilised reduced cystamine (Figs. 2 and 4). An increase in detector signal of 8622 RU was observed corresponding to approximately 8.6 ng of protein/mm^2 (Fig. 4). Lower levels of immobilisation could be obtained by reducing the injection time or the Fab′-TNB concentration. Fab′ immobilisation via thiol coupling was found to be stable with no significant loss of Fab′ fragments from the surface

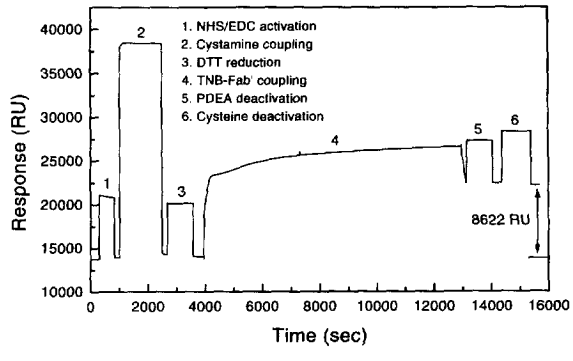

Fig. 4. Immobilisation of humanised A33 Fab′ by thiol coupling. Prior to immobilisation, Fab′ was derivatised with DTNB and purified by micropreparative SEC (see Section 2.3). Cystamine dihydrochloride was immobilised onto the carboxymethyldextran-modified gold sensor surface using NHS/EDC chemistry (stages 1, 2). After reduction with DTT (stage 3), the TNB-Fab′ was immobilised via thiol coupling onto reduced cystamine (stage 4). Residual reduced cystamine and remaining TNB active groups were deactivated by injection of 20 m*M* 2-(2-pyridinyldithio) ethane amine (PDEA) (stage 5) and 2.5 m*M* cysteine (stage 6), respectively.

observed during multiple experiments. Whilst the immobilisation of the Fab′ using the reduced cystamine–Fab′–TNB chemistry described herein proved successful, other similar immobilisation chemistries could also have been employed. Thus, using methods which have previously been described for the immobilisation of other proteins onto the biosensor, it is possible to generate a potentially very stable bond by conjugating Fab′ to immobilised *m*-maleimido benzoyl-N-hydroxysuccinimide ester (MBS) onto the sensor surface [24]. A thioether bond could also be generated by conjugating the Fab′ fragment onto a haloacetyl cross-linker [32] or a bromoacetylated spacer peptide [33] immobilised onto the sensor surface in order to achieve a more stable linkage, as has been described for diagnostic immunodetection [33].

3.6. A33 antigen binding to immobilised A33 IgG, $F(ab)'_2$ and Fab′

Varying concentrations of the purified A33 antigen (1.25–110 n*M*) were injected over the humanised A33 antibody or antibody fragments which had been immobilised onto the sensor surface using both different immobilisation chemistries and varying levels of immobilisation. It is possible to inject the same sample simultaneously over the parallel channels using the BIAcore 2000 [34]. Antigen depletion is not a problem since, even at the low n*M* level, the antigen is in large molar excess compared with the immobilised protein. A33 IgG and Fab′ were immobilised on sensor chips using different chemistries in parallel to a blank non-derivatised channel used to distinguish refractive index or non-specific binding events. Representative data are shown in Fig. 5. Binding of purified A33 antigen to A33 IgG immobilised via NHS/EDC chemistry (14.8 ng/mm^2, Fig. 5A) or cross-linked onto Protein-A (11.1 ng/mm^2, Fig. 5B) or to Fab′ immobilised via NHS/EDC (immobilisation level 8.6 ng/mm^2, Fig. 5C) and the thiol chemistry (8.6 ng/mm^2, Fig. 5D) were analysed with the same aliquot of purified protein.

3.7. The effect of the immobilisation chemistry on relative binding

It can be seen from the sensorgrams shown in Fig. 5 that the binding of the A33 ligand is greater in the channels immobilised using the methods designed to give a specific surface orientation. However for an absolute comparison to be made it is necessary to take into account the amount of antibody immobilised. The molar binding activities [27] were calculated as described in Section 2.7. These relative binding levels for the A33 antigen with immobilised IgG and Fab′ are shown in Tables 1 and 2, respectively. The data shown in these tables are representative of a number of binding studies made using different preparations of ligand and with different levels of antibody immobilisation.

The antigen responses for the A33 IgG immobilised via Protein-A cross-linking, despite the possibility of the modification of lysine residues by dimethyl pimelimidate, is 2- to 3-fold higher compared to the NHS chemistry at all levels of immobilisation (Table 1). The molar binding activities ranged from 0.18 to 0.25 for A33 IgG orientated via Protein-A and from 0.06 to 0.10 for A33 IgG conjugated by amine coupling over the antigen concentration tested. Similarly, the antigen responses for the Fab′ fragment immobilised via the SH chemistry (8.6 ng/mm^2 immobilised) is also higher (1.5- to 2-fold increase) compared with the NHS chemistry (6.4 ng/mm^2 and 2.4 ng/mm^2 immobilised) (Table 2). The molar binding activities were approximately 0.12 for Fab′ orientated via SH chemistry and ranged from 0.05 to 0.08 for Fab′ conjugated using NHS/EDC. A major advantage of the increase in reactivity observed with the surface orientation of the antibody is a concomitant increase in overall sensitivity of detection which facilitates low level analysis. This is readily evident for the lowest levels of antigen tested (cf. Fig. 5A and B, Fig. 5C and D).

Immobilisation of IgG via the Fc domain or of the Fab′ via the SH of the hinge region appeared to give a preferred orientation of antibody compared to multi-site attachment using amine coupling chemistry. Indeed, the conventional NHS/EDC chemistry which can couple by both the N-terminus and lysine residues is likely to generate multiple orientations of the antibody on the sensor surface which may compromise or mask the antibody binding domains. The humanised A33 antibody has 5 lysine residues in the light chain variable region (residues 24, 39, 45, 103 and 107) [16] and 3 in the heavy chain (residues

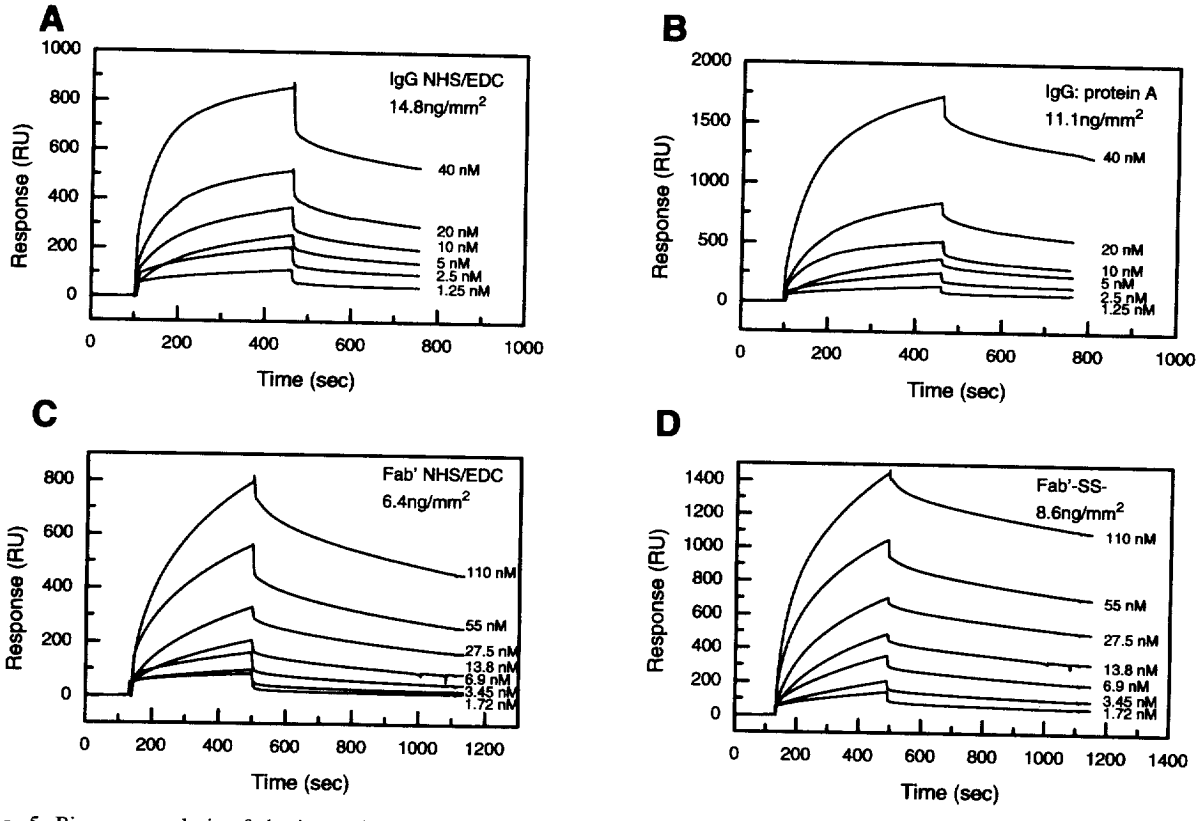

Fig. 5. Biosensor analysis of the interaction of HPLC purified A33 antigen with immobilised IgG and Fab'. Varying concentrations (1.25–110 n*M*) of the purified A33 antigen were injected (30 μl) at a flow-rate of 5 μl/min over the humanised A33 antibody or antibody fragments which had been immobilised onto the sensor surface using different immobilisation chemistries. Following the injection cycle, dissociation in BIAcore buffer was monitored for 360 s. (A) A33 antigen binding onto IgG immobilised using NHS/EDC chemistry (surface concentration: 14.8 ng/mm^2). (B) A33 antigen binding onto IgG cross-linked to Protein-A (surface concentration: 11.1 ng/mm^2). (C) A33 antigen binding onto Fab' immobilised using NHS/EDC chemistry (surface concentration: 6.4 ng/mm^2). (D) A33 antigen binding onto Fab' immobilised using thiol coupling (surface concentration: 8.6 ng/mm^2).

Table 1
Relative binding levels of A33 antigen with A33 IgG immobilised via either NHS/EDC chemistry or cross-linking onto immobilised Protein-A

A33 antigen concentration (n*M*)	IgG immobilised (ng/mm^2)	Immobilisation chemistry	Detector signal (RU)	Relative response (RU/ng/mm^2)	Molar binding activity
20	11.1	Protein-A	700	63[a]	0.22
20	14.8	NHS/EDC	392	27[b]	0.09
20	6.9	Protein-A	491	71	0.25
20	15.0	NHS/EDC	437	29	0.10
22.5	3.4	Protein-A	173	51	0.18
22.5	2.8	NHS/EDC	50	18	0.06

[a] Derived from data shown in Fig. 5A.
[b] Derived from data shown in Fig. 5B.
Other data are derived from sensorgrams not shown.

Table 2
Relative binding levels of A33 antigen with A33 Fab′ immobilised via either NHS/EDC chemistry or thiol coupling via reduced cystamine

A33 antigen concentration (nM)	Fab′ immobilised (ng/mm^2)	Immobilisation chemistry	Detector signal (RU)	Relative response (RU/ng/mm^2)	Molar binding activity
62	8.6	Thiol	859	100	0.12
62	6.4	NHS/EDC	439	69	0.08
62	2.4	NHS/EDC	152	63	0.07
55	8.6	Thiol	838	97[a]	0.11
55	6.4	NHS/EDC	409	64[b]	0.07
55	2.4	NHS/EDC	108	45	0.05

[a] Derived from data shown in Fig. 5C.
[b] Derived from data shown in Fig. 5D.
Other data are derived from sensorgrams not shown.

43, 64 and 75) [35]. Kinetic analysis of the curves was therefore performed to investigate differences in binding affinity with the different surfaces.

3.8. Kinetic analysis of the interaction between the A33 antigen and A33 IgG, F(ab)′$_2$ and Fab′

It has been shown recently that the method of analysis can influence interpretation of complex binding kinetics [22,36]. The apparent association rate (k_a) and dissociation rate (k_d) constants were therefore calculated using both non-linear least squares regression (NLLS) and linear transformation of the primary data (LR) for the analysis of the sensorgrams.

3.9. Analysis of the kinetic rate constants for the interaction between A33 antigen and A33 IgG immobilised onto Protein-A or by NHS/EDC chemistry

3.9.1. Linear analysis

The k_a and k_d were determined following linear transformation of the primary data. This treatment assumes that the A33 antigen–ligand interaction is pseudo first order. A data set generated at different concentrations is required for the determination of k_a by LR analysis. A plot of k_s (slope of the plot of dR/dt against R from the association phase of the sensorgram [21]) against concentration was generated from the data shown in Fig. 5A and B. Using this analysis, values of $k_a = 3.14 \cdot 10^5\ M^{-1}\ s^{-1}$ and $k_d = 6.77 \cdot 10^{-3}\ s^{-1}$ were obtained for A33 IgG immobilised using NHS/EDC chemistry and $k_a = 2.42 \cdot 10^5\ M^{-1}\ s^{-1}$ and $k_d = 3.52 \cdot 10^{-3}\ s^{-1}$ for A33 IgG immobilised using Protein-A. However, the k_d value obtained from LR analysis of the association phase can be prone to error, particularly when the k_d values are low [37] since k_d is usually small in relation to k_aC, and slight errors in the slope will have large effects on the measured intercept. The k_d was therefore also determined at each concentration tested by linear regression analysis of the dissociation phase data [2]. To determine regions of the curve where kinetic data could be readily extracted, and to avoid areas which are influenced by mass transport effects [38], rebinding [20,39], or complex multi-order kinetics [26], regions were selected from the sensorgrams which were linear with respect to plots of ln (R_0/R) versus t. The k_d was obtained from the slope of the resultant line. Values ranging from $1.63–1.91 \cdot 10^{-3}\ s^{-1}$ (average $1.74 \cdot 10^{-3}\ s^{-1}$) were obtained using the NHS/EDC chemistry and $1.92–2.13 \cdot 10^{-3}\ s^{-1}$ (average $2.00 \cdot 10^{-3}\ s^{-1}$) when the IgG was immobilised via Protein-A (Table 3).

3.9.2. Non-linear least squares analysis

The regions of the dissociation phase which were linear for plots of ln (R_0/R) versus t were also used for NLLS analysis [3]. The k_d was determined for each concentration tested (Table 3), resulting in values of $1.44–1.92 \cdot 10^{-3}\ s^{-1}$ (average $1.62 \cdot 10^{-3}\ s^{-1}$) for IgG immobilised via NHS chemistry, and values of $1.80–2.26 \cdot 10^{-3}\ s^{-1}$ (average $1.95 \cdot 10^{-3}\ s^{-1}$) for IgG cross-linked onto Protein-A.

It can be seen that the values of k_d obtained by LR and NLLS analysis were in good agreement, were similar over a range of concentrations suggesting that

Table 3
Linear analysis (LR) and non-linear least squares analysis (NLLS) of dissociation rate constants

Concentration (nM)	IgG NHS/EDC				IgG Protein-A				Concentration (nM)	Fab′ NHS/EDC				Fab′Thiol coupling			
	LR		NLLS		LR		NLLS			LR		NLLS		LR		NLLS	
	$k_d \times 10^3$ (M^{-1})	R^2	$k_d \times 10^3$ (M^{-1})	χ^2	$k_d \times 10^3$ (M^{-1})	R^2	$k_d \times 10^3$ (M^{-1})	χ^2		$k_d \times 10^3$ (M^{-1})	R^2	$k_d \times 10^3$ (M^{-1})	χ^2	$k_d \times 10^3$ (M^{-1})	R^2	$k_d \times 10^3$ (M^{-1})	χ^2
40	1.63	0.990	1.44	0.19	2.13	0.998	2.26	0.31	110	2.17	1.0	2.15	0.06	1.68	0.999	1.67	0.08
20	1.73	0.993	1.56	0.31	1.98	0.999	1.87	0.45	55	2.07	0.998	2.13	0.03	1.35	0.999	1.34	0.02
10	1.68	0.991	1.55	0.44	1.93	0.998	1.83	0.37	27.5	2.23	0.997	2.18	0.05	1.33	0.997	1.36	0.02
5.0	1.83	0.992	1.69	0.38	1.92	0.994	1.83	0.15	13.75	3.01	0.988	2.28	0.08	1.56	0.995	1.48	0.05
2.5	1.67	0.988	1.53	0.15	1.97	0.989	1.80	0.08	6.9	4.35	0.988	2.65	0.03	1.95	0.992	1.54	0.02
1.25	1.91	0.983	1.92	0.07	2.09	0.964	2.14	0.11	3.45	6.55	0.979	2.79	0.05	2.75	0.994	2.75	0.01

Table 4
Analysis of association rate constants by NLLS

Concentration (nM)	IgG NHS/EDC		IgG Protein-A		Concentration (nM)	Fab′ NHS/EDC		Fab′ Thiol coupling	
	$k_a \times 10^{-5}$ (M^{-1} s^{-1})	χ^2	$k_a \times 10^{-5}$ (M^{-1} s^{-1})	χ^2		$k_a \times 10^{-5}$ (M^{-1} s^{-1})	χ^2	$k_a \times 10^{-5}$ (M^{-1} s^{-1})	χ^2
40	4.49	0.35	3.85	1.40	110	1.05	0.53	3.26	0.19
20	5.17	2.08	4.02	2.41	55	1.12	0.30	3.76	1.08
10	5.67	0.04	4.86	0.83	27.5	1.38	0.68	3.18	0.03
5.0	5.36	0.04	4.86	0.03	13.75	1.32	0.93	3.50	0.04
2.5	4.85	0.05	4.52	0.05	6.9	1.22	0.67	3.46	0.13
1.25	4.67	0.06	3.89	0.08	3.45	4.08	0.55	3.99	0.08

rebinding was not significant over the regions of the sensorgrams analysed and displayed good fitting as shown by the values of R^2 and χ^2 (Table 3). These values of k_d were therefore used to constrain the analysis of k_a by NLLS, as well as for the calculation of the equilibrium association constant, K_A.

The regions of the association phase of the sensorgrams, which were linear with respect to plots of ln dR/dt versus t and which had previously been used to determine the values of k_s in the LR analysis, were used for the NLLS analysis of k_a (Table 4). The single exponential form of the rate equation [3] was used. Although using this method it is possible to determine the rate constants from a single sensorgram obtained with a known concentration of ligand, each concentration tested was analysed individually to check for any significant variation of the rate constants. The k_a values determined at each concentration were similar yielding values of $4.49–5.67 \cdot 10^5$ M^{-1} s^{-1} (average $5.03 \cdot 10^5$ M^{-1} s^{-1}) for IgG immobilised via NHS chemistry, and values of $3.85–4.86 \cdot 10^5$ M^{-1} s^{-1} (average $4.27 \cdot 10^5$ M^{-1} s^{-1}) for IgG cross-linked onto Protein-A (Table 4).

3.10. Analysis of the kinetic rate constants for the interaction between A33 antigen and A33 Fab′ immobilised by thiol coupling or NHS/EDC chemistry

A similar approach to that described in Section 3.9 for analysis of the interaction between the A33 antigen and A33 IgG was used for the analysis of the interaction with the A33 Fab′ fragment. LR analysis of the association phase data yielded a k_a of $3.37 \cdot 10^5$ M^{-1} s^{-1} ($R^2 = 0.998$) for the Fab′ immobilised using the thiol coupling method and a value of $1.46 \cdot 10^5$ M^{-1} s^{-1} ($R^2 = 0.999$) for the NHS/EDC chemistry (Table 5). LR analysis of the dissociation phase data for the thiol immobilisation surface gave values of $1.33–1.68 \cdot 10^{-3}$ s^{-1} for the k_d obtained at concentrations between 13.75–110 nM (average $1.48 \cdot 10^{-3}$ s^{-1}) (Table 3). However at the two lowest A33 antigen concentrations tested slightly higher values were calculated (1.95 and $2.75 \cdot 10^{-3}$ s^{-1}).

Using the NHS/EDC immobilisation chemistry the off rate appeared faster, with values of $2.07–2.23 \cdot 10^{-3}$ s^{-1} being determined from data generated

Table 5
Summary of the kinetic analysis of the biosensor binding data for A33 antigen–humanised A33 mAb interactions

	k_a (LR) $\times 10^{-5}$ (M^{-1} s^{-1})	k_d (LR) $\times 10^3$ (s^{-1})	K_A (LR) $\times 10^{-8}$ (M^{-1})	k_a (NLLS) $\times 10^{-5}$ (M^{-1} s^{-1})	k_d (NLLS) $\times 10^3$ (s^{-1})	K_A (NLLS) $\times 10^{-8}$ (M^{-1})
IgG (NHS)	3.14	1.74	1.80	5.03	1.62	3.10
IgG (Protein-A)	2.42	2.00	1.21	4.27	1.95	2.18
$F(ab')_2$ (NHS)	0.88	1.60	0.55	0.78	1.66	0.47
Fab′ (NHS)	1.46	2.16	0.67	1.20	2.15	0.56
Fab′ (SH)	3.37	1.48	2.27	3.52	1.48	2.37

between 27.5–110 nM (average $2.16 \cdot 10^{-3}$ s^{-1}). As had been observed using the thiol coupling chemistry, an apparent dependence on concentration was noted at the lower concentrations (Table 3).

The differences in k_d observed between the two immobilisation chemistries were confirmed by NLLS analysis. Using this method, values of $1.34–1.67 \cdot 10^{-3}$ s^{-1} (average $1.14 \cdot 10^{-3}$ s^{-1}) were calculated for the thiol surface over the concentration range 6.9–110 nM and $2.13–2.28 \cdot 10^{-3}$ s^{-1} (average $2.15 \cdot 10^{-3}$ s^{-1}) for the amine coupling chemistry between 27.5 and 110 nM (Table 3). These values are in good agreement with those calculated for the corresponding curves by LR analysis (Table 3). Whilst NLLS also indicated variations in the off rate at lower concentrations, the effect was not as great with the NHS/EDC chemistry as had been suggested by the LR analysis.

To confirm that the variations in k_d observed were not due to rebinding, experiments were performed in which excess soluble A33 Fab′ was injected during the dissociation phase [20]. These experiments (data not shown) gave similar values for k_d to those determined at the higher concentrations when buffer alone was flowing over the sensor surface during the dissociation phase, when rebinding would be expected to be minimal.

NLLS analysis of the association phase, using the average values of k_d calculated above to constrain the calculation, yielded values of $3.18–3.99 \cdot 10^5$ M^{-1} s^{-1} (average $3.52 \cdot 10^5$ M^{-1} s^{-1}) for the k_a when the thiol coupling chemistry was used (Table 4). The corresponding analysis of the NHS/EDC surface gave a k_a of $1.05–1.38 \cdot 10^5$ M^{-1} s^{-1} (average $1.2 \cdot 10^5$ M^{-1} s^{-1}) for concentrations above 6.9 nM, although the value appeared almost 4-fold higher at the lowest concentration tested (Table 4). However this may well be due to the low signal which was being analysed. It is interesting to note that the same sample passed over the surface generated by the thiol coupling chemistry, where a more responsive surface was obtained, did not show this deviation.

3.11. Analysis of the kinetic rate constants for the interaction between A33 antigen and A33 F(ab)′$_2$ immobilised using the NHS/EDC chemistry

The A33 F(ab′)$_2$ fragment was only immobilised using the NHS/EDC chemistry due to the absence of the Fc domain or free SH group. However, we have analysed the kinetic data to enable a comparison of the relative rate constants of the antibody and antibody fragments using a "standard" chemistry. Additionally, since the F(ab′)$_2$ was used to generate the Fab′ for the immobilisation it was important to determine whether the affinity had been significantly modified during the proteolytic digestion. Using LR analysis a value of $8.8 \cdot 10^4$ M^{-1} s^{-1} was calculated for the k_a. The k_d, derived from the analysis of the initial regions of the dissociation phase, ranged between 1.36–1.98 s^{-1} (average $1.60 \cdot 10^{-3}$ s^{-1}) over the concentration range tested (Table 5). Using NLLS, values of 1.41–1.89 s^{-1} (average $1.66 \cdot 10^{-3}$ s^{-1}) were determined for the k_d. The k_a values determined at each concentration ranged from $6.29 \cdot 10^4$ M^{-1} s^{-1} at the lowest concentration tested to $9.71 \cdot 10^4$ M^{-1} s^{-1} (average $7.58 \cdot 10^4$ M^{-1} s^{-1}) for the data generated with 155 nM A33 antigen.

4. Conclusions

The BIAcore 2000 biosensor, which uses the optical detection principle of surface plasmon resonance, was used to study the interactions between the HPLC purified A33 antigen and the humanised A33 IgG, F(ab)′$_2$ or Fab′ fragments immobilised onto the sensor surface. The conventional NHS/EDC chemistry, which can couple by both the N-terminus and lysine residues, is likely to generate multiple orientations of the antibody which can induce surface heterogeneity, alter binding characteristics and create complex kinetics. Alternative chemistries were therefore designed to give a defined spatial orientation of IgG and Fab′ on the sensor surface which should result in optimum presentation of the antibody for A33 antigen binding. These chemistries (Protein-A cross-linking for IgG, thiol conjugation for Fab′) were found to generate surfaces which were stable to the regeneration conditions used, and showed no significant bleeding during prolonged use.

Surface orientation immobilisation gave higher molar binding activities for both IgG (2- to 3-fold higher) and Fab′ fragment (1.5- to 2-fold increase) compared with the NHS chemistry. This resulted in a concomitant increase in overall sensitivity of detection which facilitates low level analysis.

Protein-A immobilisation gives similar binding kinetics for the A33 ligand to the IgG when compared to the immobilisation using NHS/EDC. This may be due to the relatively large number of lysine residues in the Fc region of the molecule [35], which may tend to immobilise the antibody without interfering with the binding site. Indeed, the affinity constant obtained with the Protein-A immobilisation, calculated from values obtained using either LR or NLLS analysis, appeared slightly lower suggesting that the dimethyl pimelimidate cross-linking may have slight adverse effects by modifying lysine residues in the variable region of the molecule.

The generation of $F(ab)'_2$ and Fab′ fragments followed by immobilisation using NHS/EDC chemistry resulted in significant reduction in the apparent affinity (Table 5). This could be due to either partial denaturation caused by the enzymatic digestion or by a more pronounced effect of the immobilisation via lysine residues than had been observed with the intact IgG molecule. However, in the case of Fab′ immobilisation using thiol coupling, kinetic analysis of the binding curves showed a faster on and slower off rate than had been observed with the NHS/EDC chemistry. This resulted in a similar equilibrium constant (K_A) for the Fab′ to that observed for the intact IgG suggesting modification of the lysine residues during NHS/EDC immobilisation was responsible for the lower activity observed with this chemistry.

A further extension of these studies is that, for the generation of Fab′ immunoconjugates for clinical use, the conjugation via the SH group of the hinge region may well be the method of choice. This will result in a controlled conjugation and will avoid multiple site attachment which, as shown herein, can reduce biological activity.

Similar biosensor analyses will be used to evaluate such immunoconjugates developed for immunotherapy and tumour localisation studies as well as the detection of the A33 antigen in circulating cells, physiological fluids and fecal washings.

References

[1] M. Malmqvist, Nature, 361 (1993) 186.

[2] R. Karlsson, A. Michaelsson and L.J. Mattsson, Immunol. Methods, 145 (1991) 229.

[3] D.J. O'Shannessy, M. Brigham-Burke, K.K. Soneson, P. Hensley and I. Brooks, Anal. Biochem., 212 (1993) 457.

[4] B. Liedberg, I. Lundstom and E. Stenberg, Sensors Actuators, 11 (1993) 63.

[5] S. Löfas and B. Johnsson, J. Chem. Soc., Chem. Commun., 21 (1990) 1526.

[6] S. Welt, C.R. Divgi, F.X. Real, S.D. Yeh, P. Garin-Chesa, C.L. Finstad, J. Sakamoto, A. Cohen, E.R. Sigurdson, N. Kemeny, E.A. Carswell, H.F. Oettgen and L.J. Old, J. Clin. Oncol., 8 (1990) 1894.

[7] S. Welt, C.R. Divgi, N. Kemeny, R.D. Finn, A.M. Scott, M. Graham, J. St. Germain, E. Carswell Ricards, S.M. Larson, H.F. Oettgen and L.J. Old, J. Clin. Oncol., 12 (1994) 1561.

[8] S. Welt, A.M. Scott, C.R. Divgi, N. Kemeny, R.D. Finn, F. Daghighian, J. St. Germain, E. Carswell Ricards, S.M. Larson and L.J. Old, J. Clin. Oncol., 14 (1996) 1787.

[9] B. Catimel, G. Ritter, S. Welt, L.J. Old, L. Cohen, M.A. Nerrie, S.J. White, J.K. Heath, B. Demediuk, T. Domagala, F.T. Lee, A.M. Scott, H. Ji, R.L. Moritz, R.J. Simpson, A.W. Burgess and E.C. Nice, J. Biol. Chem., 41 (1996) 25 664.

[10] R.H. Whitehead, F.A. Macrae, D.J.B. St. John and J. Ma, J. Natl. Cancer Inst., 74 (1985) 759.

[11] E.C. Nice, M. Lackmann, F. Smyth, L. Fabri and A.W. Burgess, J. Chromatogr. A, 660 (1994) 169.

[12] G. Ritter, R.L. Moritz, H. Ji, L. Cohen, E. Nice, B. Catimel, J.K. Heath, S. Welt, A.W. Burgess, L.J. Old and R.J. Simpson, in preparation.

[13] E.C. Nice, Nature, 348 (1990) 462.

[14] E.C. Nice, L. Fabri, A. Hammacher, K. Andersson and U. Hellman, Biomed. Chrom., 7 (1993) 104.

[15] E.C. Nice, Biopolymers, 40 (1996) 319.

[16] D.J. King, P. Antoniw, R.J. Owens, J.R. Adair, A.M.R., Haines, A.P.H. Farnsworth, H. Finney, A.D.G. Lawson, A. Lyons, T.S. Baker, D. Baldock, J. Mackintosh, C. Gofton, G.T. Yarranton, W. McWilliams, D. Shochat, P.K. Leichner, S. Welt, L.J. Old and A. Mountain, Br. J. Cancer, 72 (1995) 1364.

[17] C. Schneider, R.A. Newman, D.R. Sutherland, U. Asser and F.G. Melvyn, J. Biol. Chem., 257 (1982) 10 766.

[18] K.M. Wilson, M. Gerometta, D.B. Rylatt, P.G. Bundesen, D.A. McPhee, C.J. Hillyard and B.E. Kemp, J. Immunol. Methods, 138 (1991) 111.

[19] P. Parham, J. Immunol., 131 (1983) 2895.

[20] G. Panayotou, G. Gish, P. End, O. Truong, I. Gout, R. Dhand, M.J. Fry, I. Hiles, T. Pawson and M.D. Waterfield, Mol. Cell. Biol., 13 (1993) 3567.

[21] R. Karlsson, D. Altschuh and M.H.V. Van Regenmortel, in Structure of Antigens, CRC Press, Boca Raton, FL, 1992, p. 127.

[22] E.C. Nice, T.L. McInerney and D.C. Jackson, Mol. Immunol., 33 (1996) 659.

[23] B. Johnsson, S. Löfas and G. Lindquist, Anal. Biochem., 198 (1991) 268.

[24] D.J. O'Shannessy, M. Brigham-Burke and K. Peck, Anal. Biochem., 205 (1992) 132.

[25] S. Löfas, B. Johnsson, A. Edström, A. Hansson, G. Lindquist, R.M. Müller Hillgren and L. Stigh, Biosensors Bioelectronics, 10 (1995) 813.

[26] R. Karlsson, H. Roos, L. Fagerstam and B. Persson, in Methods: A Companion to Methods in Enzymol., 6 (1994) 99.
[27] B. Johnsson, S. Löfas, G. Lindquist, A. Edstrom, R.M. Müller Hillgren and A. Hansson, J. Mol. Recognit., 8 (1995) 125.
[28] E.C. Nice, J. Layton, L. Fabri, U. Hellman, A. Engstrom, B. Persson and A.W. Burgess, J. Chromatogr., 646 (1993) 159.
[29] B. Johne, K. Hansen, E. Mork and J. Holtlund, J. Immunol. Methods, 183 (1995) 167.
[30] A. Bernard and R. Bosshard, Eur. J. Biochem., 230 (1995) 416.
[31] E. Stenberg, B. Persson, H. Roos and C. Urbaniczky, J. Colloid Interface Sci., 43 (1990) 513.
[32] M. Brinkley, Bioconj. Chem., 3 (1992) 2.
[33] K.M. Wilson, B. Catimel, K. Mitchelhill and B.E. Kemp, J. Immunol. Methods, 175 (1994) 267.
[34] R. Karlsson, J.A. Mo and R. Holmdahl, J. Immunol. Methods, 188 (1995) 63.
[35] N. Takahashi, S. Udea, M. Obata, T. Nikaido, S. Nakai and T. Honjo, Cell, 29 (1982) 671.
[36] T.A. Morton, D.G. Myszka and I.M. Chaiken, Anal. Biochem., 227 (1995) 176.
[37] I.M. Chaiken, S. Rose and R. Karlsson, Anal. Biochem., 201 (1992) 197.
[38] R.W. Glaser, Anal. Biochem., 213 (1993) 152.
[39] G. Payne, S.E. Shoelson, G.D. Gish, T. Pawson and C.T. Walsh, Proc. Natl. Acad. Sci. USA, 90 (1993) 4902.